

## Mechanistic Studies on the Formation of Linear Polyethylene Chain Catalyzed by Palladium Phosphine–Sulfonate Complexes: Experiment and Theoretical Studies

Shusuke Noda,<sup>†</sup> Akifumi Nakamura,<sup>†</sup> Takuya Kochi,<sup>†,§</sup> Lung Wa Chung,<sup>‡</sup> Keiji Morokuma,<sup>\*,‡</sup> and Kyoko Nozaki<sup>\*,†</sup>

*Department of Chemistry and Biotechnology, Graduate School of Engineering, The University of Tokyo, 7-3-1 Hongo, Bunkyo-Ku, Tokyo 113-8656, Japan, and Fukui Institute for Fundamental Chemistry, Kyoto University, Takano-Nishishiraki-cho, 34-4, Sakyo-ku, Kyoto 606-8103, Japan*

Received June 15, 2009; E-mail: nozaki@chembio.t.u-tokyo.ac.jp

**Abstract:** Linear polyethylene propagation starting from Pd phosphine–sulfonate complexes, Pd(CH<sub>3</sub>)(L)(Ar<sub>2</sub>PC<sub>6</sub>H<sub>4</sub>SO<sub>3</sub>) (L = 2,6-lutidine, Ar = *o*-MeOC<sub>6</sub>H<sub>4</sub> (**2a**) and L = pyridine, Ar = Ph (**2b**)), was studied both experimentally and theoretically. Experimentally, highly linear polyethylene was obtained with Pd(CH<sub>3</sub>)(L)(Ar<sub>2</sub>PC<sub>6</sub>H<sub>4</sub>SO<sub>3</sub>) complexes **2a** and **2b**. Formation of a long alkyl-substituted palladium complex (**3**) was detected as a result of ethylene oligomerization on a palladium center starting from methylpalladium complex. Additionally, well-defined ethyl and propyl complexes (**6<sub>Et</sub>** and **6<sub>Pr</sub>**) were synthesized as stable *n*-alkyl palladium complexes. In spite of the existence of β-hydrogens, the β-hydride elimination to give 1-alkenes was very slow or negligible in all cases. On the other hand, isomerization of 1-hexene in the presence of a methylpalladium/phosphine–sulfonate complex **2a** indicated that this catalyst system actually undergoes β-hydride elimination and reinsertion to release internal alkenes. On the theoretical side, the relative energies were calculated for intermediates and transition states for chain-growth, chain-walking, and chain-transfer on the basis of the starting model complex Pd(*n*-C<sub>3</sub>H<sub>7</sub>)(pyridine)(*o*-Me<sub>2</sub>PC<sub>6</sub>H<sub>4</sub>SO<sub>3</sub>) (**8**). First, *cis/trans* isomerization process via the Berry's pseudorotation was proposed for the Pd/phosphine–sulfonate system. The second oxygen atom of sulfonate group is involved in the isomerization process as the associative ligand, which is one of the most unique natures of the sulfonate group. Chain propagation was suggested to take place from the less stable alkylPd(ethylene) complex **10'** with the TS of 27.4/27.7 ((*E*+ZPC)/*G*) kcal/mol. Possible β-hydride elimination was suggested to occur under low concentration of ethylene: the highest-energy transition state to override for β-hydride elimination was either >37.4/25.3 kcal/mol (TS(**9-12**)) or 29.1/27.4 kcal/mol (TS(**8'-9'**)) to reach **12'**. The ethylene insertion to the *iso*-alkylpalladium species (**14'**) is allowed via a TS of 28.6/29.1 kcal/mol (TS(**14'-15'**)), slightly higher in energy than that for the *normal*-alkylpalladium species (TS(**10'-11'**)). Easy chain transfer was suggested to proceed from the more stable PdH(olefin) complex **12'** if β-hydride elimination to **12'** does take place. Thus, the production of linear polyethylene with high molecular weight under ethylene pressure suggests that the *cis* and *trans* PdH(alkene)(phosphine–sulfonate) complexes (**12** and **12'**) are merely accessible in the presence of excess amount of ethylene.

### Introduction

Group 4 transition metal catalysts play the major role in industrial production of linear high-density polyethylene (HDPE). On the other hand, significant efforts have been intensively devoted in the past decade to developing late transition-metal catalysts for ethylene polymerization, since they were considered to be potentially capable of producing copolymers of ethylene and readily available polar olefins by coordination polymerization.<sup>1</sup> Using α-diimine palladium complexes, Brookhart reported the coordination copolymerization of ethylene with methyl acrylate to produce highly branched copolymers in

1996.<sup>2</sup> The branched structure was suggested to arise from so-called “chain walking”, that is, rapid β-hydride elimination from a *normal*-alkylmetal intermediate giving a hydridometal–olefin complex, reinsertion of the olefin to the metal–hydride bond providing *iso*-alkylmetal species, and chain growth from the *iso*-alkylmetal complex.

In 2002, a group at Shell laboratory reported the synthesis of linear copolymers of ethylene and alkyl acrylates using *in situ* generated Pd catalysts by admixture of palladium precursor

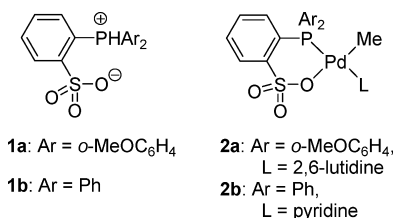
- (1) (a) Ittel, S. D.; Johnson, L. K.; Brookhart, M. *Chem. Rev.* **2000**, *100*, 1169–1203. (b) Gibson, V. C.; Spitzmesser, S. K. *Chem. Rev.* **2003**, *103*, 283–315. (c) Boffa, L. S.; Novak, B. M. *Chem. Rev.* **2000**, *100*, 1479–1493. (d) Sen, A.; Borkar, S. *J. Organomet. Chem.* **2007**, *692*, 3291–3299.
- (2) (a) Johnson, L. K.; Mecking, S.; Brookhart, M. *J. Am. Chem. Soc.* **1996**, *118*, 267–268. (b) Mecking, S.; Johnson, L. K.; Wang, L.; Brookhart, M. *J. Am. Chem. Soc.* **1998**, *120*, 888–899.

<sup>†</sup> The University of Tokyo.

<sup>‡</sup> Kyoto University.

<sup>§</sup> Present address: Department of Chemistry, Faculty of Technology, Keio University, 3-14-1 Hiyoshi, Kohoku-ku, Yokohama, Kanagawa 223-8522, Japan.

and phosphonium–sulfonate **1a**.<sup>3</sup> As the copolymer thus obtained can be considered as a functionalized HDPE, the report attracted much attention from both academia and industry. Since then, incorporation of several common polar vinyl monomers to linear polyethylene were reported for acrylates,<sup>4–6</sup> acrylonitrile,<sup>7</sup> vinyl fluoride,<sup>8</sup> vinyl ethers,<sup>9</sup> and others.<sup>10,11</sup> Among the late transition-metal catalysts, the first-row transition metal such as Ni, Fe, and Co were usually used to obtain linear polyethylenes.<sup>12</sup> In contrast, few available examples of Pd catalyst can produce linear polyethylene, and these limited examples require the presence of activators, such as MAO.<sup>13</sup> It should be noted that the Pd phosphine–sulfonate complexes are active without using any activators or noncoordinating counterions.



In order to elucidate the above-mentioned unique properties of the catalyst system, the reaction mechanism of ethylene polymerization catalyzed by the Pd phosphine–sulfonate system was studied both experimentally<sup>5–7,10,14</sup> and theoretically.<sup>15</sup> By using the theoretical approach, Ziegler et al. reported that the  $\beta$ -hydride elimination is slower compared to the polymer-chain growth in the catalyst system.<sup>15</sup> On the contrary, occurrence of chain walking via repetitive  $\beta$ -hydride elimination and reinsertion of the olefin was suggested by Jordan et al. on the basis of microstructure analysis of the polymers and their observation of  $\beta$ -chloride elimination from  $\omega$ -chloroalkylpalladium species.<sup>14</sup> The  $\beta$ -hydride elimination–reinsertion process was also suggested by Claverie based on their observation of 1-octene isomerization into internal octenes.<sup>10</sup> Concurrently, we found

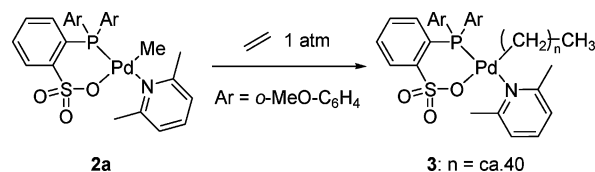
another  $\beta$ -hydride elimination pathway with lower energy (TS(**9'**–**12'**) in Figure 8) during our preliminary calculations on the basic reactions of this system. This apparent contradiction prompted us for further studies on the ethylene polymerization using Pd phosphine–sulfonate complexes. Here we report our independent study on the polyethylene synthesis by using catalyst **2** both experimentally and theoretically. We isolated and characterized the growing ethylene chain on the isolated methylpalladium complex **2a**. In addition, our detailed theoretical calculations revealed that the concentration of ethylene may control the molecular weight and the microstructure of the polyethylene product.

## Results and Discussions

### 1. Characterization of Alkylpalladium Complexes of Phosphine–Sulfonate as an Intermediate to Provide Linear Polyethylene.

Formation of linear polyethylene by using palladium complex derived from phosphonium–sulfonate **1a** was recently reported by several research groups.<sup>5–7,10,14</sup> The results we independently examined with methylpalladium lutidine complex **2a** are shown in Table S-1 in Supporting Information. In addition, we prepared methylpalladium complex **2b** having phenyl groups on phosphorus atom and pyridine as the forth ligand. Under ethylene pressure of 3.0 MPa in 15 h in toluene, highly linear polyethylene was obtained. Higher catalytic activity and molecular weight were observed with **2a** (15 g·mmol<sup>−1</sup> h<sup>−1</sup>, *M<sub>n</sub>* 63000) than **2b** (7.3 g·mmol<sup>−1</sup> h<sup>−1</sup>, *M<sub>n</sub>* 6000). Here we report our observation of polyethylene chain growth on the palladium center by NMR spectroscopy, which accords with the coordination polymerization mechanism. When a solution of complex **2a** in CDCl<sub>3</sub> was treated with 1.0 atm of ethylene in an NMR tube, formation of a palladium complex **3** bearing a linear long alkyl chain was detected (Scheme 1).

#### Scheme 1. Formation of Long Alkyl Complex



All the peaks of <sup>1</sup>H NMR chart were unambiguously characterized by COSY (Figure 1) and <sup>1</sup>H{<sup>31</sup>P} NMR (Figure S-1 in Supporting Information). Palladium–lutidine complex **3** was detected as a predominant species accompanied by 3.5% of the corresponding palladium–ethylene complex, Pd(alkyl)-(CH<sub>2</sub>=CH<sub>2</sub>)(Ar<sub>2</sub>PC<sub>6</sub>H<sub>4</sub>SO<sub>3</sub>), the values being calculated based on <sup>1</sup>H NMR peaks for coordinating ethylene ( $\delta$  4.91–5.02) and for free lutidine ( $\delta$  2.52). The methylene protons at the  $\beta$ - and  $\gamma$ -positions of palladium exhibited their peaks with unexpectedly high-field shift,  $\delta$  0.43 and 0.47, respectively (*vide infra*). The long Pd–alkyl complex **3** was reasonably stable even in the absence of ethylene. No change was detected for complex **3** in a solid state for several days, but slow decomposition was observed in a halogenated solvent. In a chloroform or dichloroethane solution, chloropalladium complex **4** was formed as a result of replacement of the alkyl group by chloride (Scheme 2). This decomposition may have occurred via homolytic scission of the palladium–carbon bond followed by the abstraction of a chlorine atom from the halogenated solvent by the palladium center radical. The structure of complex **4** was confirmed by X-ray single crystal analysis (Tables S2–S7, Supporting Information).

- (3) Drent, E.; van Dijk, R.; van Ginkel, R.; van Oort, B.; Pugh, R. I. *Chem. Commun.* **2002**, 744–745.
- (4) Kochi, T.; Yoshimura, K.; Nozaki, K. *Dalton Trans.* **2006**, 25–27.
- (5) Skupov, K. M.; Marella, P. R.; Simard, M.; Yap, G. P. A.; Allen, N.; Conner, D.; Goodall, B. L.; Claverie, J. P. *Macromol. Rapid Commun.* **2007**, *28*, 2033–2038.
- (6) Guironnet, D.; Roesle, P.; Rünzi, T.; Göttker-Schnetmann, I.; Mecking, S. *J. Am. Chem. Soc.* **2009**, *131*, 422–423.
- (7) Kochi, T.; Noda, S.; Yoshimura, K.; Nozaki, K. *J. Am. Chem. Soc.* **2007**, *129*, 8948–8949.
- (8) Weng, W.; Shen, Z.; Jordan, R. F. *J. Am. Chem. Soc.* **2007**, *129*, 15450–15451.
- (9) Luo, S.; Vela, J.; Lief, G. R.; Jordan, R. F. *J. Am. Chem. Soc.* **2007**, *129*, 8946–8947.
- (10) Skupov, K. M.; Piche, L.; Claverie, J. P. *Macromolecules* **2008**, *41*, 2309–2310.
- (11) Borkar, S.; Newsham, D. K.; Sen, A. *Organometallics* **2008**, *27*, 3331–3334.
- (12) (a) Kuhn, P.; Semeril, D.; Matt, D.; Chetcuti, M. J.; Lutz, P. *Dalton Trans.* **2007**, 515–528. (b) Younkin, T. R.; Conner, E. F.; Henderson, J. I.; Friedrich, S. K.; Grubbs, R. H.; Bansleben, D. A. *Science* **2000**, *287*, 460–462. (c) Gibson, V. C.; Redshaw, C.; Solan, G. A. *Chem. Rev.* **2007**, *107*, 1745–1776.
- (13) (a) Tsuji, S.; Swenson, D. C.; Jordan, R. F. *Organometallics* **1999**, *18*, 4758–4764. (b) Li, K. L.; Darkwa, J.; Guzei, I. A.; Mapolie, S. F. *J. Organomet. Chem.* **2002**, *660*, 108–115. (c) Mohlala, M. S.; Guzei, I. A.; Darkwa, J.; Mapolie, S. F. *J. Mol. Catal. A: Chem.* **2005**, *241*, 93–100. (d) Chen, R.; Mapolie, S. F. *J. Mol. Catal. A: Chem.* **2003**, *193*, 33–40.
- (14) Vela, J.; Lief, G. R.; Shen, Z.; Jordan, R. F. *Organometallics* **2007**, *26*, 6624–6635.
- (15) Haras, A.; Anderson, G. D. W.; Michalak, A.; Rieger, B.; Ziegler, T. *Organometallics* **2006**, *25*, 4491–4497.

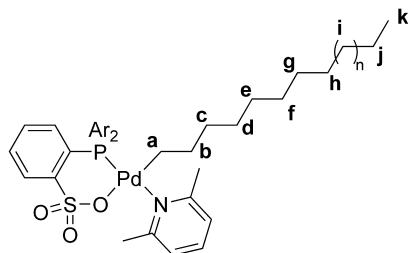
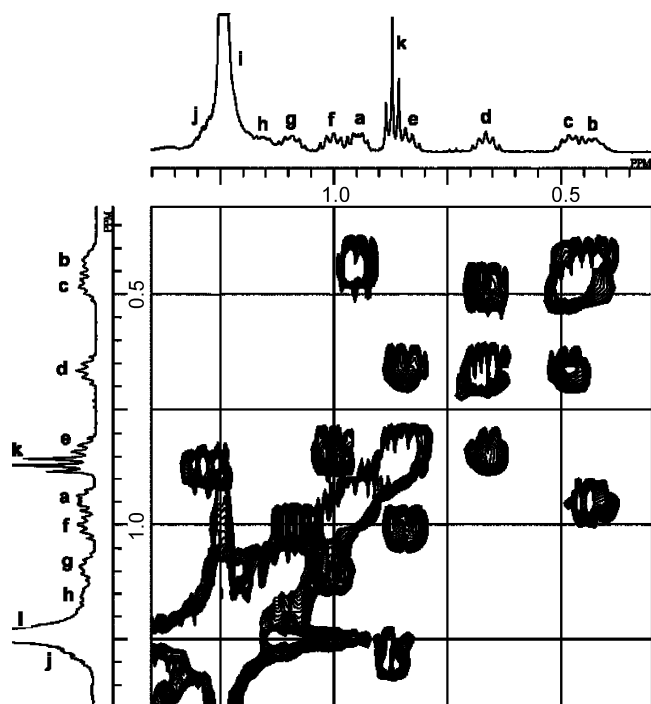
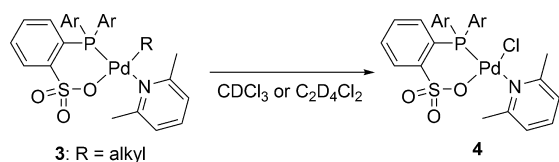


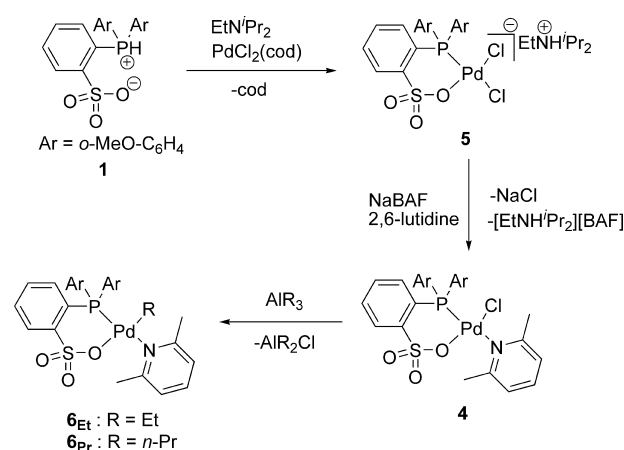
**Figure 1.** Formation of **3** from **2a** and ethylene (HH COSY in  $\text{CDCl}_3$ ).

**Scheme 2.** Decomposition of Alkyl Complex



The high stability of the long Pd-alkyl complex **3** encouraged us to prepare an alkyl palladium complex with a certain carbon number. The precursors, dichloropalladium **5** and chloropalladium(lutidine) **4** were easily prepared following to Scheme 3. The preparation of ethyl and *n*-propyl complexes **6<sub>Et</sub>** and **6<sub>Pr</sub>** are achieved by the transmetalation reaction of trialkylaluminum species with chloropalladium **4**.<sup>16</sup> The monoalkyl complexes were isolated as yellow solids in moderate yields. As shown in the NMR spectra of **6<sub>Et</sub>**, the peak for the  $\alpha$ -methylene protons was detected at  $\delta$  1.02 and that for the  $\beta$ -methyl protons at  $\delta$  0.00 (Figure 2, bottom). These values are upfield shifted, compared to the peaks reported for ethylpalladium(phenanthroline)(pyridine) complex:<sup>17</sup>  $\delta$  2.04 for

**Scheme 3.** Synthesis of Alkyl Complexes **6<sub>Et</sub>** and **6<sub>Pr</sub>**



the  $\alpha$ -methylene and  $\delta$  0.95 for the  $\beta$ -methyl. Both  $\alpha$ - and  $\beta$ -protons coupled with the phosphorus atom as were confirmed by  $^1\text{H}\{^31\text{P}\}$  NMR (Figure 2). In *n*-propyl complex **6<sub>Pr</sub>**, the  $\gamma$ -methyl protons were also observed at higher field,  $\delta$  0.17 (Figure 3, bottom). Observation of the *n*-propyl complex **6<sub>Pr</sub>** is in sharp contrast to the report by Brookhart showing isomerization of a *normal*-propylpalladium complex to an *iso*-propylpalladium under even  $-110$  °C in the absence of additional Lewis base (2,6-lutidine in our case).<sup>18</sup> In complex **6<sub>Pr</sub>**, not only the  $\alpha$ - and  $\beta$ -methylene protons, but the  $\gamma$ -carbon coupled with the phosphorus atom ( $J_{\text{P-C}} = 4$  Hz). In both complexes **6<sub>Et</sub>** and **6<sub>Pr</sub>**, the methyl proton peak for free 2,6-lutidine (2.5 ppm) was not observed.

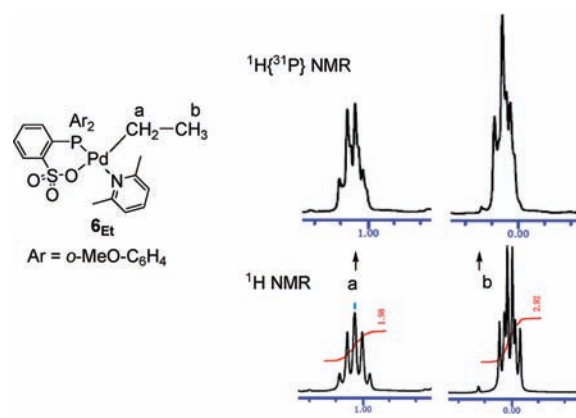


**Figure 2.**  $^1\text{H}$  and  $^1\text{H}\{^31\text{P}\}$  NMR spectra of **6<sub>Et</sub>** (in  $\text{CDCl}_3$ ).

One possible reason for the upfield shift of  $\alpha$ - $\gamma$  protons and the P-H and P-C couplings in **6<sub>Et</sub>** and **6<sub>Pr</sub>** may be attributed to shield effect by aromatic rings of the ligand. Another possibility is an agostic interaction of one of the C-H bonds with the metal center represented as Scheme 4. In fact, the contribution of the  $\beta$ - or  $\gamma$ -agostic alkylpalladium species accompanied by lutidine dissociation was suggested by the following experiment. Addition of extra amount of 2,6-lutidine to a solution of complex **3** generated from **6<sub>Pr</sub>** resulted in the disappearance of the peak(s) around  $\delta$  0.50.

(16) Considering our theoretical studies in this paper, the stability of **6<sub>Et</sub>** and **6<sub>Pr</sub>** may be explained by the following two possibilities. (1)  $\beta$ -hydride elimination from **6<sub>Et</sub>** or **6<sub>Pr</sub>** (corresponds to **TS(9-12)** and/or **TS(8'-9')**) is slow under the conditions for our NMR studies. (2) The *normal*-complex **6<sub>Pr</sub>** is more stable than its *iso*-alkyl isomer (an analogue of **13+pyridine**) due to the bulkiness of the ligand **1a** and of the lutidine.

(17) Milani, B.; Marson, A.; Scarel, A.; Ernsting, G. M. M.; Elsevier, C. J. *Organometallics* **2004**, *23*, 1974–1977.

(18) (a) Shultz, L. H.; Tempel, D. J.; Brookhart, M. *J. Am. Chem. Soc.* **2001**, *123*, 11539–11555. (b) Tempel, D. J.; Johnson, L. K.; Huff, R. L.; White, P. S.; Brookhart, M. *J. Am. Chem. Soc.* **2000**, *122*, 6686–6700.

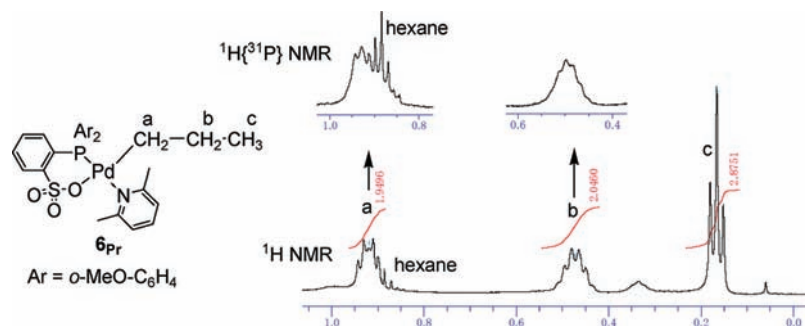


Figure 3.  $^1\text{H}$  and  $^1\text{H}\{^{31}\text{P}\}$  NMR spectra of  $6_{\text{Pr}}$  (in  $\text{CDCl}_3$ ).

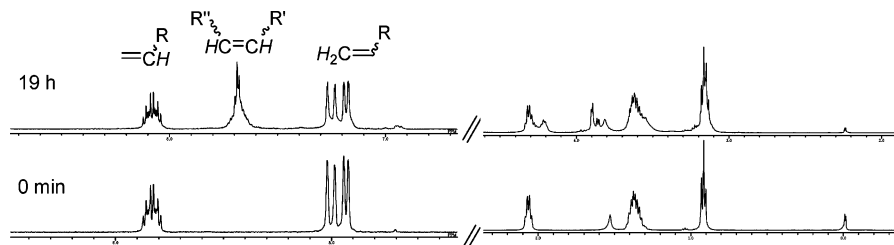
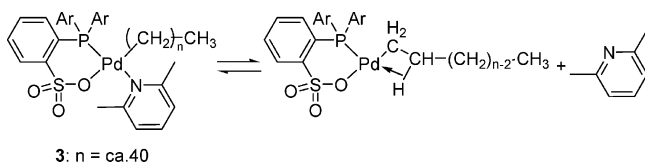


Figure 4. Isomerization of 1-hexene ( $^1\text{H}$  NMR in  $\text{C}_2\text{D}_4\text{Cl}_2$ ).

**Scheme 4.** Dissociation of 2,6-Lutidine from **3** As a Possible Reason for the Up-Field Shift



**2. Isomerization of 1-Hexene in the Presence of Complex 2a.** When a solution of methylpalladium complex **2a** (0.010 mmol) in 0.5 mL of  $\text{C}_2\text{D}_4\text{Cl}_2$  was treated with 13 equivalent amount of 1-hexene in an NMR tube, a terminal olefin was slowly converted to internal olefins (Figure 4). After 19 h at 60 °C, 63% (7.8 mmol) of the 1-hexene was converted to internal olefins. Most likely, this transformation was caused by terminal olefin insertion to a palladium–carbon or palladium–hydrogen bond followed by  $\beta$ -hydride elimination. Thus, it is proven that the  $\beta$ -hydride elimination does proceed with this catalyst system, at least in the absence of ethylene.<sup>10</sup> At the same time,  $^{31}\text{P}$  NMR spectrum shows several peaks including 24.5 ppm which corresponds to the *normal*-hexylpalladium complex  $6_{\text{Hex}}$  (24  $\mu\text{mol}$ , after 19 h) generated by 1,2-insertion of 1-hexene into a Pd–H bond. In other words, the *normal*-alkyl complex  $6_{\text{Hex}}$  exists as a stable species as complex **3**. The chloropalladium complex **4** gradually appeared probably via the radical decomposition process (38  $\mu\text{mol}$ , after 19 h) (Figure 5).

### 3. Results of Theoretical Calculations

In our theoretical studies, density functional theory (B3LYP<sup>19/6-31G\*</sup> and LanL2dz<sup>20</sup>) was employed. As a model for calculations, the palladium/phosphine–sulfonate complex **2** was simplified as **7** with replacement of the aryl groups on phosphorus atom by methyl groups and 2,6-lutidine by pyridine (Figure 6).

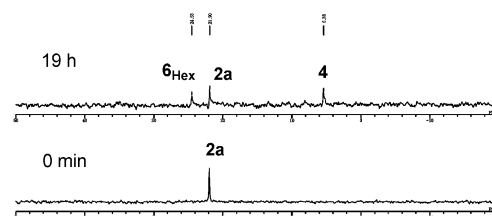


Figure 5. Formation of *n*-hexyl complex  $6_{\text{Hex}}$  starting from complex **2a** ( $^{31}\text{P}$  NMR in  $\text{C}_2\text{D}_4\text{Cl}_2$ ).

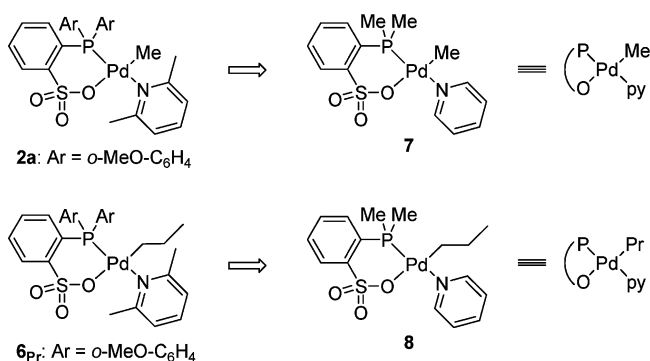
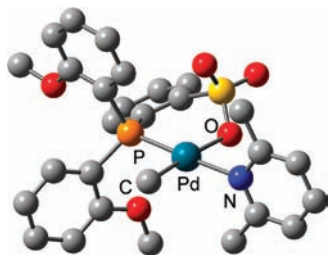


Figure 6. Simplified structure of phosphine–sulfonate palladium complexes.

The propyl complex  $6_{\text{Pr}}$  was simplified as **8**,<sup>21</sup> and the relative energies ( $E+\text{ZPC}$ , with zero point energy correction, before /) and free energies ( $G$ , after /) for all the stationary points will be expressed relative to the complex **8** in the following studies. Complexes with phenyl groups on the phosphorus atom were also employed to study some of the key steps (labeled with a subscript of Ph, such as  $8_{\text{Ph}}$ ). Complexes with **Ph** suffix should be considered as real species because complex **2b** did produce linear polyethylene as was described in the former part of this

(19) (a) Becke, A. D. *J. Chem. Phys.* **1993**, *98*, 5648–5652. (b) Lee, C.; Yang, W.; Parr, R. G. *Phys. Rev. B* **1988**, *37*, 785–789.  
(20) Hay, P. J.; Wadt, W. R. *J. Chem. Phys.* **1985**, *82*, 270–283.

(21) Additionally, we found that Pd complexes bearing alkylphosphine–sulfonate ligands are also effective catalysts for the production of highly linear polyethylene. See Supporting Information.



**Figure 7.** Optimized structure of **2a**. The hydrogen atoms are omitted for clarity.

**Table 1.** Selected Bond Lengths and Angles of **2a** Determined by the X-ray Crystallography and Calculations (in parentheses)

bond	length [Å]	angle	[deg]
Pd–C	2.134 (2.056)	C–Pd–N	88.66 (91.71)
Pd–N	2.134 (2.181)	N–Pd–O	89.99 (84.77)
Pd–O	2.159 (2.190)	O–Pd–P	95.00 (93.54)
Pd–P	2.234 (2.311)	P–Pd–C	86.44 (89.99)
		C–Pd–O	178.53 (175.65)
		P–Pd–N	173.29 (178.19)

**Table 2.** Substituents Effect on the Relative Energies of Some Key Intermediates and Transition States (kcal/mol)

with Me	E+ZPE	H	G	with Ph	E+ZPE	H	G
<b>8</b>	0.0	0.0	0.0	<b>8<sub>Ph</sub></b>	0.0	0.0	0.0
<b>TS(8'–9')</b>	29.1	29.2	27.4	<b>TS(8'<sub>Ph</sub>–9'<sub>Ph</sub>)</b>	28.6	28.9	26.0
<b>TS(9'–10')</b>	33.0	32.8	30.9	<b>TS(9'<sub>Ph</sub>–10'<sub>Ph</sub>)</b>	32.2	32.0	30.3
<b>TS(10'–11')</b>	27.4	26.1	27.7	<b>TS(10'<sub>Ph</sub>–11'<sub>Ph</sub>)</b>	26.8	25.7	26.1
<b>TS(9–9')</b>	44.5	44.1	31.7	<b>TS(9<sub>Ph</sub>–9'<sub>Ph</sub>)</b>	42.2	41.8	28.9
<b>TS(9–12)</b>	no TS found			<b>TS(9<sub>Ph</sub>–12<sub>Ph</sub>)</b>	36.4	35.9	24.5
<b>TS(9'–12')</b>	31.5	31.0	19.9	<b>TS(9'<sub>Ph</sub>–12'<sub>Ph</sub>)</b>	30.7	30.4	18.4
<b>TS(14'–15')</b>	28.6	27.4	29.1	<b>TS(14'<sub>Ph</sub>–15'<sub>Ph</sub>)</b>	28.0	26.8	28.8
<b>19'</b>	43.0	42.8	19.4	<b>19'<sub>Ph</sub></b>	42.9	42.9	18.6
<b>TS(12'–17')</b>	24.6	24.1	24.2	<b>TS(12'<sub>Ph</sub>–17'<sub>Ph</sub>)</b>	26.0	25.5	25.8

paper. The optimized structure of **2a** was in reasonable agreement with the X-ray crystal structure,<sup>7</sup> as shown in Figure 7 and Table 1.

The processes we studied include *cis/trans* isomerization of palladium phosphine-sulfonate complexes (section 3.1), chain-propagation reaction to form linear polyethylene (section 3.2),  $\beta$ -hydride elimination reactions (section 3.3), chain-propagation reaction to form branched-polyethylene (section 3.4), chain transfer reaction to release 1-alkene (section 3.5), and calculations for representative intermediates and transition states with the real system (section 3.6). The representative data of the real system relative to **8<sub>Ph</sub>** are summarized in Table 2 in section 3.1. The overall calculated energy profile for sections 3.1–3.4 is summarized in Figure 8 for perspective. After the calculation results in sections 3.1–3.6, we will discuss the overall reaction, especially focusing on Routes 1–3 in Figure 8, in order to clarify why Pd phosphine-sulfonate catalysts can produce highly linear polyethylene, selectively.

**3.1. *cis/trans* Isomerization of Four-Coordinate and  $\beta$ -Agostic Three-Coordinate Pd Phosphine-Sulfonate Complexes and Their Stability.** Due to the unsymmetric character of the phosphine-sulfonate bidentate ligand, *cis/trans* isomerization should be considered for  $\beta$ -agostic *cis*-alkyl complex **9** as well as for four-coordinate complexes such as *cis*-alkylPd(pyridine) complex **8** and *cis*-alkylPd(ethylene) complex **10**.<sup>22</sup> Here in this study, we have revealed that the sulfonate group plays a unique role to facilitate the isomerization. The *cis/trans* isomerization mechanisms of square-planar palladium complexes were well

studied.<sup>23,24</sup> One possible pathway is a simple geometry change via tetrahedral four-coordinate species (Scheme 5, rotation A). In fact, we could locate tetrahedral transition state (**TS(10–10')**tetrahedral) for *cis/trans* isomerization between the alkylPd(ethylene) complexes **10** and **10'**, which is 19.3/20.3 kcal/mol above complex **10**.

Another possible *cis/trans* isomerization of the square-planar palladium complexes is an associative pathway which is accompanied by ligand association–substitution reactions.<sup>23</sup> In this case, five-coordinate structures can be considered as transition states for such isomerization. Our trials to locate a transition state for isomerization of **10** to **10'** involving an external ethylene as the fifth ligand resulted in a simple dissociation of ethylene. *Instead, for the Pd phosphine-sulfonate system, we found that the second oxygen atom of the sulfonate group is involved in the isomerization process as the associative ligand* (Scheme 5, rotation B). For instance, *cis/trans* isomerization process from *cis*-alkylPd(ethylene) complex **10** to its *trans*-isomer **10'** was facilitated by simultaneous exchange of oxygen atoms of the SO<sub>3</sub> group. The geometry of this transition state **TS(10–10')** resembles square pyramidal where the phosphorus atom is located at the apical position. This **TS(10–10')** involving the SO<sub>3</sub>-rotation is 15.9/16.1 kcal/mol above **10** (Scheme 5), which is lower than the simple rotation TS (19.3/20.3 kcal/mol) discussed in the previous paragraph. This rotation pattern (Scheme 5, rotation B) via five-coordinate complex is recognized as “Berry’s pseudorotation” based on the TS structure.<sup>25</sup> Similar to **TS(10–10')**, we have successfully found *cis/trans* isomerization pathway through **TS(9–9')** (Scheme 7) from **9** to **9'** with exchanging oxygen atoms of sulfonate group. The agostic hydrogen atom has interaction to the metal center in **TS(9–9')**. The geometry of this transition state is also similar to square pyramidal where the phosphorus atom is located at the apical position. As another possibility for isomerization from **9** to **9'**, one may consider the dissociation–isomerization pathway, that is a loss of agostic C–H interaction and isomerization from one T-shape structure to another.<sup>23</sup> Nevertheless, we could not find such processes between the alkylpalladium complexes **9** and **9'**.

The *cis/trans* isomerization from **8** to **8'** was also searched. In this case, we found that the reaction takes place in two steps (Scheme 6) with an intermediate (**8med**), as was confirmed by intrinsic reaction coordinate (IRC) calculations. In the course of **8** → **TS(8–8med)** → **8med** → **TS(8med–8')** → **8'**, the oxygen atoms of the SO<sub>3</sub> group exchanged. For both **8** and **9**, TSs via simple rotation via tetrahedral four-coordinate species were also calculated giving higher barriers than the TSs for isomerization with SO<sub>3</sub> rotation.

Isomerization pathway via dissociation of the sulfonate group from the metal center is less probable. Dissociation of the SO<sub>3</sub>

(22) Although *cis/trans* isomerization reactions of a series of Pd phosphine-sulfonate complexes were proposed by Ziegler et al. in reference 15 the structures of the TSs were not fully reported. See also: (a) Haras, A.; Michalak, A.; Rieger, B.; Ziegler, T. *J. Am. Chem. Soc.* **2005**, *127*, 8765–8774. (b) Haras, A.; Michalak, A.; Rieger, B.; Ziegler, T. *Organometallics* **2006**, *25*, 946–953.

(23) Anderson, G. K.; Cross, R. *J. Chem. Soc. Rev.* **1980**, *9*, 185–215.

(24) For some examples of the studies on *cis/trans* isomerization reactions of square-planar Pd complexes, see: (a) Deubel, D. V.; Ziegler, T. *Organometallics* **2002**, *21*, 4432–4441. (b) Frankcombe, K. E.; Cavell, K. J.; Yates, B. F.; Knott, R. B. *Organometallics* **1997**, *16*, 3199–3206. (c) Casares, J. A.; Espinet, P. *Inorg. Chem.* **1997**, *36*, 5428–5431. (d) Casares, J. A.; Espinet, P. *Inorg. Chem.* **1998**, *37*, 2096.

(25) Ugi, I.; Marquard, D.; Klusacek, H.; Gillespi, P.; Ramirez, F. *Acc. Chem. Res.* **1971**, *4*, 288–296. (a) See also references 24c and d.

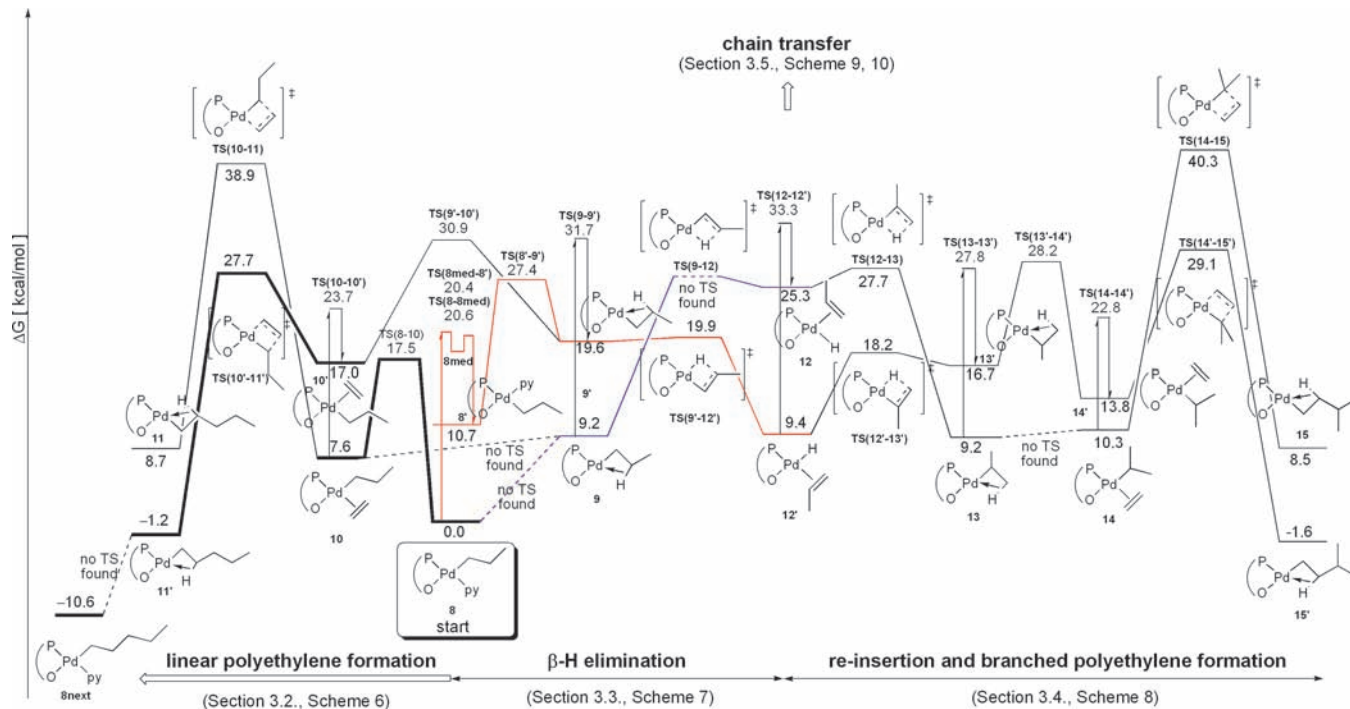
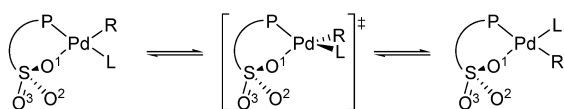


**Figure 8.** Energy profile for chain propagation to give linear and branched alkyl chain, and  $\beta$ -hydride elimination from alkyl Pd species. The Gibbs free energies (in kcal/mol) relative to **8** are given. **Bold:** Route 1, Blue: Route 2, Red: Route 3 in Discussion section (Scheme 11).

**Scheme 5.** Two Possible Routes for Isomerization of Pd Phosphine–Sulfonate Complexes

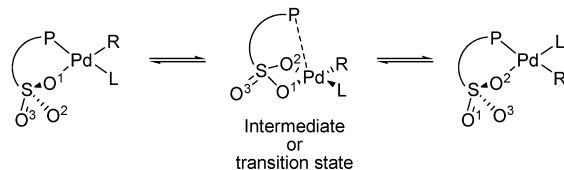
**rotation A**

"simple rotation via tetrahedral TS"



**rotation B**

"rotation via Berry's Pseudorotation-like TS"



group from the complex **8** provided a three-coordinate intermediate at quite high energy level (**8-SO<sub>3</sub>away**, 31.7/29.7 kcal/mol from **8**, see Supporting Information). The rigid structure of the phenylene backbone of the bidentate ligand seems to prevent dissociation of the SO<sub>3</sub> group.

These isomerization processes **TS(8-8')**, **TS(9-9')**, and **TS(10-10')** require rather similar energy barriers from their reactants **8**, **9**, and **10**. However, the relative energies of these TSs based on the complex **8** are different because relative stability of the reactants **8**, **9**, and **10** are not equal. Therefore, some isomerization can proceed, while the others cannot, as will be discussed below. Other *cis/trans* isomerizations, namely, **TS(12-12')**, **TS(13-13')**, and **TS(14-14')** (Scheme 8) were also found to occur with rotation of the sulfonate group. These TSs will appear in the following sections without detailed discussions. For more structural information, see Supporting Information.

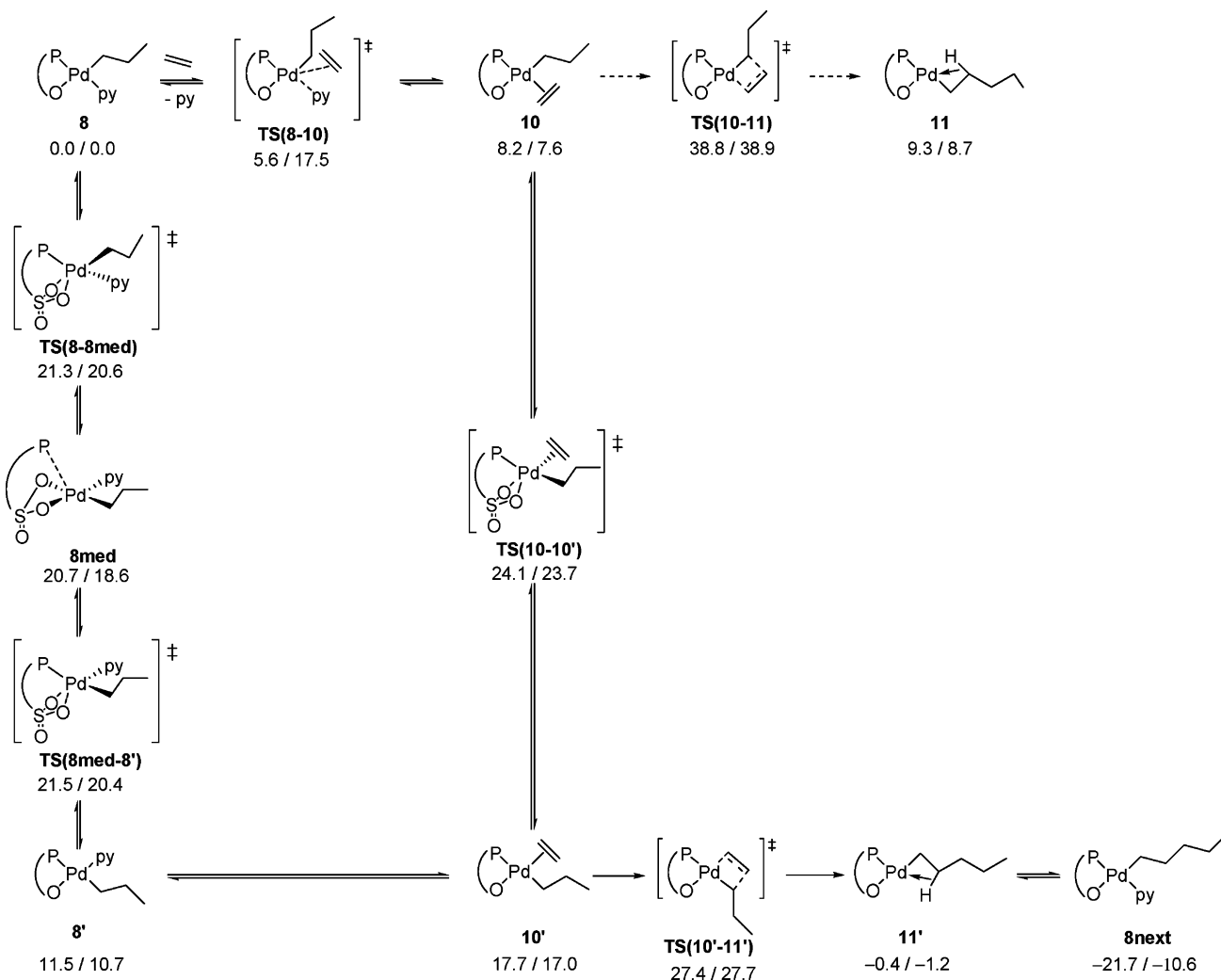
For all pairs of *cis/trans* isomers in the intermediates, it is apparent from Figure 8 that the alkyl group or hydrogen atom located *trans* to oxygen is favored over their isomers. This is

in agreement with the X-ray analyses of the reported Pd phosphine–sulfonate complexes.<sup>4–7,14</sup> This preference can be attributed to the strong *trans* influence of alkyl group, hydrogen atom, and phosphine moiety which dislike being *trans* to each other.<sup>14,22</sup>

**3.2. Chain-Propagation Reaction to Form Linear Polyethylene.** Chain-propagation reaction proceeds via Cossee mechanism including olefin insertion into the metal–carbon bond. Four-membered ring transition states for ethylene insertion were calculated for two isomeric ethylene complexes **10** and **10'** to produce **11** and **11'**, respectively. Possible intermediates and transition states for the ethylene insertion to the carbon–palladium bond starting from the propyl complex **8** are drawn in Scheme 6. First, replacement of pyridine by ethylene takes place by an associative mechanism via **TS(8-10)** (5.6/17.5 kcal/mol). As described in the previous section, *cis/trans* isomerization is possible from **10** to **10'**. Although the isomer **10** is lower in energy than the other isomer **10'**, the transition state **TS(10-11)** for ethylene insertion is higher than the other transition state **TS(10'-11')** by 11.4/11.2 kcal/mol. Lower energy of **TS(10'-11')** can be attributed to the stronger *trans* effect of the phosphine moiety than the sulfonate oxygen. Because olefin insertion is recognized as the migration of alkyl group to the ethylene, the strong *trans* effect of the phosphorus atom should enhance the migrating ability of the alkyl group leading to the rapid insertion. Accordingly, the propyl group in **10** undergoes isomerization to form the more reactive isomer **10'** with the alkyl group *trans* to the phosphine via **TS(10-10')**.<sup>26,27</sup> Although

(26) Similar results were obtained in the case of other olefin polymerization catalysts bearing unsymmetric bidentate ligands. For example, (a) Chan, M. S. W.; Deng, L. Q.; Ziegler, T. *Organometallics* **2000**, *19*, 2741–2750. (b) Michalak, A.; Ziegler, T. *Organometallics* **2003**, *22*, 2069–2079. (c) See also references 15, 22a,b, and 24a.

(27) More detailed analysis on ethylene insertion regarding the nature of the unsymmetric character of this ligand is described in Supporting Information.

Scheme 6. Propagation Reaction for Linear Alkyl Complex ( $E+ZPE/G$ , kcal/mol)

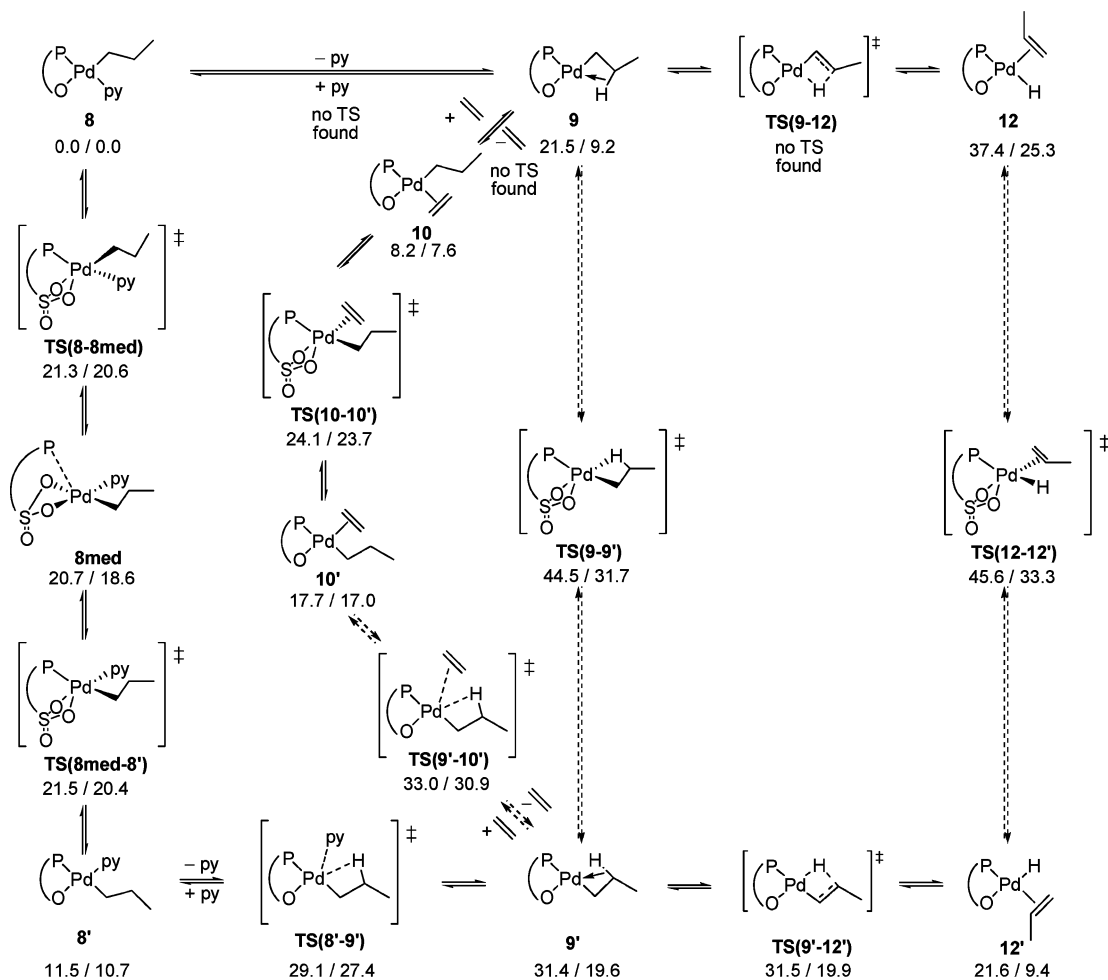
$8 \rightarrow 8_{\text{med}} \rightarrow 8' \rightarrow 10'$  is another possible route from  $8$  to  $10'$ , we omit this discussion because  $8 \rightarrow 10 \rightarrow \text{TS}(10-10') \rightarrow 10'$  is lower in energy than  $\text{TS}(10'-11')$ , anyway. Thus, processes via  $8 \rightarrow 10 \rightarrow \text{TS}(10-10') \rightarrow 10' \rightarrow \text{TS}(10'-11') \rightarrow 11'$  complete the propagation reaction.<sup>15</sup> Immediate association of pyridine to  $11'$  without barrier regenerates an alkyl pyridine complex  $8_{\text{next}}$ . In addition to  $\text{TS}(10'-11')$  for the model complex, the transition state  $\text{TS}(10'_{\text{Ph}}-11'_{\text{Ph}})$  was calculated for the realistic complex bearing phenyl groups on the phosphorus atom showing a relative energy of 26.8/26.1 kcal/mol from the starting propyl complex,  $8_{\text{Ph}}$  (Table 2).

**3.3.  $\beta$ -Hydride Elimination Reactions.** For the  $\beta$ -hydride elimination process, two pathways based on *cis/trans* isomers are considered (Scheme 7). The  $\beta$ -agostic *cis*-alkyl complex  $9$  undergoes  $\beta$ -hydride elimination to give olefin hydride complex  $12$  via transition state  $\text{TS}(9-12)$ . The C=C bond of the coordinated olefin in the complex  $12$  is perpendicular to the square-planar plane. The transition state  $\text{TS}(9-12)$  could not be located due to its very late nature and low reverse barrier: The relative energy of the  $\beta$ -elimination product  $12$  is 37.4/25.3 kcal/mol relative to  $8$ , indicating that the relative energy of  $\text{TS}(9-12)$  is equal or slightly higher than this value (Scheme 7 and Figure 8). In addition, when the two methyl groups on the phosphorus atom are replaced by phenyl groups, the transition state  $\text{TS}(9_{\text{Ph}}-12_{\text{Ph}})$  was located with the energy of 36.4/24.4 kcal/mol relative to the starting complex  $8_{\text{Ph}}$  (Table 2).

The critical issue is that the  $\beta$ -hydride elimination barrier for  $9$  or  $9_{\text{Ph}}$  is reasonably high, at least comparable to the ethylene insertion TS,  $\text{TS}(10'-11')$  (27.4/27.7 kcal/mol) or to TS calculated for the diphenylphosphino system  $\text{TS}(10'_{\text{Ph}}-11'_{\text{Ph}})$  (26.8/26.1 kcal/mol, see Table 2).

It is of interest to note that the other isomer,  $\beta$ -agostic *trans*-alkyl complex  $9'$  would undergo much lower-energy  $\beta$ -hydride elimination via transition state  $\text{TS}(9'-12')$  if  $9'$  exists. The relative energy for  $\text{TS}(9'-12')$  from  $8$  is 31.5/19.9 kcal/mol which is much lower than the other isomeric  $\text{TS}(9-12)$  by at least 5.9/5.4 kcal/mol. The lower-energy  $\text{TS}(9'-12')$  is the result of the stronger *trans* effect of the phosphorus atom than the sulfonate oxygen. The relative energy of the favorable  $\beta$ -hydride elimination TS is not strongly affected by the size of the ligand ( $\text{TS}(9'_{\text{Ph}}-12'_{\text{Ph}})$ : 30.7/18.4 kcal/mol). It should be noted, however, the reactant  $9'$  is less accessible due to the high-energy TSs to be overcome, such as  $\text{TS}(8'-9')$  (29.1/27.4 kcal/mol),  $\text{TS}(9-9')$  (44.5/31.7 kcal/mol), or  $\text{TS}(9'-10')$  (29.1/27.4 kcal/mol). In addition, the route  $9 \rightarrow 12 \rightarrow 12' \rightarrow 9'$  is also less

(28) Relative electronic energy of  $\text{TS}(8'-9')$  is lower than that of  $9'$ . This indicates the existence of another lower-energy intermediate before  $9'$ . By IRC calculation from  $\text{TS}(8'-9')$ , an intermediate which can be recognized as " $9'$  + pyridine" was obtained. In fact, the relative electronic energy of " $9'$  + pyridine" was lower than that of  $9'$ ; however, the Gibbs free energy was higher than that of  $9'$ .

Scheme 7.  $\beta$ -Hydride Elimination and Re-insertion Reactions ( $E+ZPE/G$ , kcal/mol)<sup>28</sup>

probable because *cis/trans* isomerization of **12** and **12'** needs 45.6/33.3 kcal/mol from **8**.

**3.4. Chain-Propagation Reaction to Form Branched Polyethylene.** After  $\beta$ -hydride elimination, the coordinating olefin in **12** can reinsert into the palladium hydride bond. If the reinsertion takes place with the opposite regiochemistry to the direction of **9**, branched alkyl complex **13** would be given via **TS(12-13)** (Scheme 8 and Figure 8). Although the coordinated propylene is required to rotate from perpendicular to parallel to the square planar plane in **12**, we assume that the rotation of propylene takes place with a low barrier prior to the processes **12**  $\rightarrow$  **TS(9-12)**  $\rightarrow$  **9** or **12**  $\rightarrow$  **TS(12-13)**  $\rightarrow$  **13**.<sup>29</sup> The relative energy for **TS(12-13)** was calculated to be 38.9/27.7 kcal/mol from starting **8**. The transition state connecting complexes **12'** and **13'**, **TS(12-13')**, was located at 29.8/18.2 kcal/mol.

The branched alkyl complex **13** and its isomer **13'** can bind ethylene to form the branched alkyl olefin complexes **14** and **14'**, and then migratory insertion occurs via transition states **TS(14-15)** and **TS(14'-15')**, respectively (Scheme 8). The transition state **TS(14-15)** is shown to be higher in energy (40.5/40.3 kcal/mol) than **TS(14'-15')** (28.6/29.1 kcal/mol). The relative energy for olefin insertion into the branched alkyl complex via **TS(14'-15')** is slightly higher than that into linear

alkyl complex (27.4/27.7 kcal/mol for **TS(10'-11')**) by 1.2/1.4 kcal/mol; this is even higher by 1.2/2.7 kcal/mol by using the more realistic catalyst via **TS(14'-Ph-15'-Ph)** and **TS(10'-Ph-11'-Ph)** (Table 2). The energy difference value of 1.2/2.7 kcal/mol is similar to the value reported for the cationic  $\alpha$ -diimine system.<sup>29,30</sup>

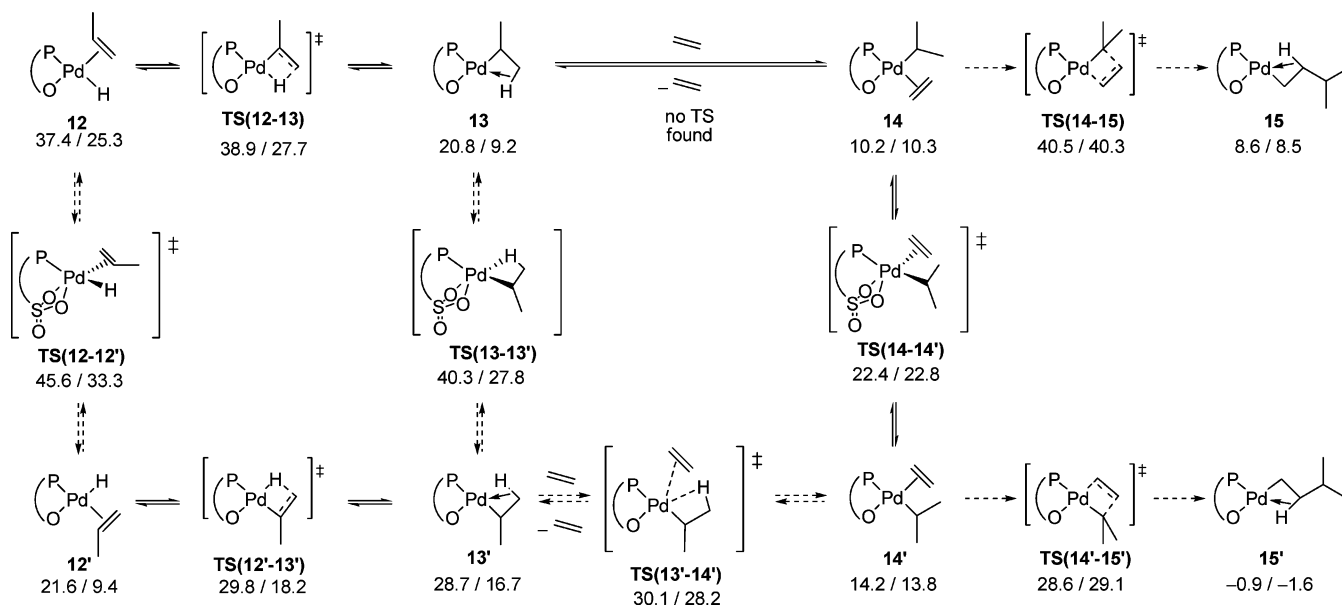
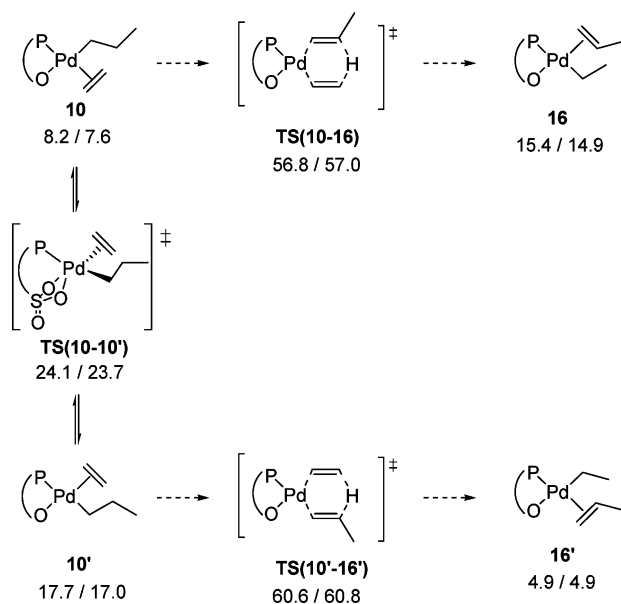
**3.5. Chain-Transfer Reaction to Release 1-Alkene.** If  $\beta$ -hydride elimination reactions from **9** to **12** or from **9'** to **12'** does take place, the chain-transfer reaction, which gives a short oligomer, should be considered. In the late transition metal catalyzed olefin polymerization, the chain transfer reactions via (i) direct  $\beta$ -hydride transfer, (ii) associative olefin displacement, and (iii) dissociative olefin displacement have been proposed.<sup>1a,29</sup>

The possibilities of (i) direct  $\beta$ -hydride transfer reactions can be excluded (Scheme 9). From the propylpalladium(ethylene) complex **10**, the direct  $\beta$ -hydride transfer reaction requires 56.8/57.0 kcal/mol to produce **16**. Similarly, the isomeric complex **10'** requires 60.6/60.8 kcal/mol to undergo the direct  $\beta$ -hydride transfer. These TSs are so high in energy that these pathways are impossible to proceed.

(29) (a) Musaev, D. G.; Svensson, M.; Morokuma, K.; Stromberg, S.; Zetterberg, K.; Siegbahn, P. E. M. *Organometallics* **1997**, *16*, 1933–1945. (b) Froese, R. D. J.; Musaev, D. G.; Morokuma, K. *J. Am. Chem. Soc.* **1998**, *120*, 1581–1587.

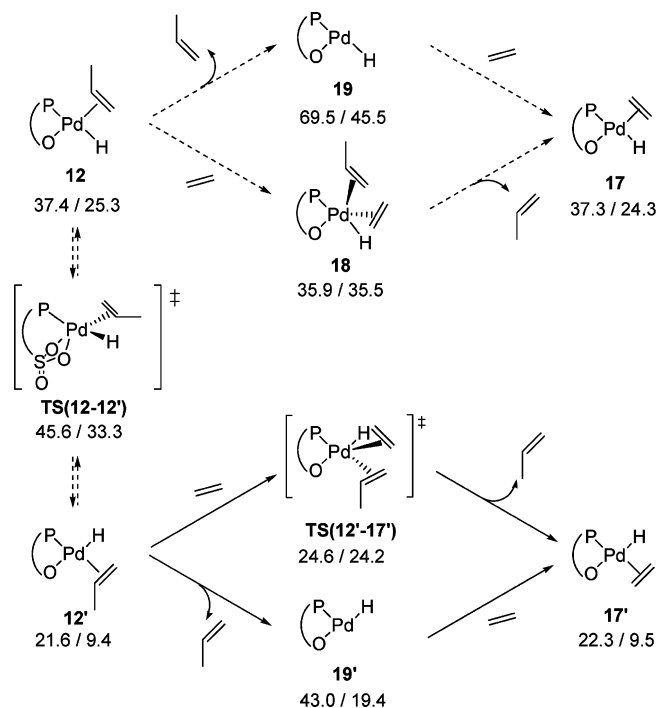
(30) One may assume that the steric demand would elevate in the ethylene insertion TS for the *iso*-alkylpalladium when the longer alkyl chain is adopted. However, the difference in **TS(10'-Ph-11'-Ph)** and **TS(14'-Ph-15'-Ph)** was quite similar if **8<sub>nextPh</sub>** was used as a starting structure instead of **8<sub>Ph</sub>**.



**Scheme 8.** Re-insertion of the Coordinating Propylene and Subsequent Ethylene Insertion into *iso*-Alkylpalladium Species (*E*+ZPE/G, kcal/mol)**Scheme 9.** Direct  $\beta$ -Hydride Transfer Reaction (*E*+ZPC/G, kcal/mol)

Associative (ii) or dissociative (iii) olefin displacement seems to happen, but only occasionally (Scheme 10). For the associative olefin displacement from **12** to **17**, the transition state **TS(12-17)** could not be located. However, a five-coordinate intermediate<sup>29</sup> **18** was found with a relative energy of 35.9/35.5 kcal/mol, suggesting that this route is less favorable. Dissociation of the olefin from **12** requires at least a relative energy of 69.5/45.5 kcal/mol or higher to give three-coordinate intermediate **19**. Thus, neither associative nor dissociative pathway for the olefin displacement from **12** can take place.

On the other hand, if the PdH(olefin) complex **12'**, the *trans* isomer of **12**, could be generated, both associative (ii) and dissociative (iii) pathways may be possible to give ethylene complex **17'**. The relative energy of a TS from **12'** to **17'** for the associative pathway was calculated to be 24.6/24.2 kcal/mol, which is lower than that for the olefin insertion via **TS(10'-**

**Scheme 10.** Associative and Dissociative Olefin Displacement As Possible Chain Transfer Processes (*E*+ZPC/G, kcal/mol)

**11'**) (27.4/27.7 kcal/mol) by 2.8/3.5 kcal/mol. The preference toward the associative olefin displacement for the realistic model via **TS(12'<sub>Ph</sub>-17'<sub>Ph</sub>)** with respect to the olefin insertion via **TS(10'<sub>Ph</sub>-11'<sub>Ph</sub>)** is reduced to 0.8/0.3 kcal/mol (Table 2). The three-coordinate PdH complex **19'** was also found to be at the relative energy of 43.0/19.4 kcal/mol, which is partly driven by a large entropy gain in the gas phase. Assuming that the dissociation of the olefin from **12'** to **19'** proceeds without barrier, the dissociative pathway is likely to take place and result in chain-transfer reaction, but it could be partly suppressed by excess amount of ethylene (*vide infra*). In summary, once the

palladium hydride complex **12'** is produced, it may undergo the chain-transfer reaction via either associative or dissociative mechanism.

**3.6. Calculations for Representative Intermediates and Transition States with the Realistic System.** Some of the critical intermediates and transition states were calculated with phenyl groups on the phosphorus atom. The energy values relative to the starting propyl complex **8<sub>Ph</sub>** were summarized in Table 2. In addition to the values  $\Delta E + ZPE$  and  $\Delta G$ ,  $\Delta H$  is also listed. It should be emphasized that the differences in relative energies between the simplified ligand (Me groups on phosphorus) and the real ligand (Ph groups on phosphorus) are negligible. As we previously mentioned in this manuscript, complex **2b** with the ligand bearing Ph groups on the phosphorus atom and pyridine as the fourth ligand produced highly linear polyethylene (*vide supra*).<sup>21</sup>

Furthermore, instead of the combination of 6-31G\* and LanL2dz, some important intermediates and transition states were also tested by larger triple- $\zeta$  basis sets plus polarization and diffuse functions, 6-311+G\*\* and SDD+f (see Supporting Information).<sup>31</sup> In addition, solvent effect was also considered by PCM calculation using toluene as a solvent which is actually employed in polymerization experiments (see Supporting Information). According to the results with larger basis sets and PCM calculation, some relative energies were changed; however, these differences did not alter the interpretation of the calculation discussed below.

**3.7. Discussions on the Theoretical Studies Sections 3.1–3.6.** The chain-growth, chain-walking, and chain-transfer mechanisms were studied starting from a model complex **8**. In section 3.1, a unique *cis/trans* isomerization process was proposed for the Pd phosphine–sulfonate system, via the so-called “Berry’s pseudorotation”. The second oxygen atom of sulfonate group is involved in the isomerization process as the associative ligand to lower the transition state compared to a simple rotation mechanism. The isomerization was accompanied by simultaneous exchange of oxygen atoms of the SO<sub>3</sub> group at the transition state. We believe that this is one of the most characteristic features of a sulfonate group, which differentiate the phosphine–sulfonate ligand from other anionic bidentate ligands. For all pairs of *cis/trans* isomers in the intermediates, the alkyl group or hydrogen atom located *trans* to oxygen is favored over their isomers. This preference can be attributed to the strong *trans* influence of alkyl group, hydrogen atom, and phosphine moiety which dislike being *trans* to each other.

In section 3.2, chain propagation was suggested to take place from the less stable *cis*-alkylPd(ethylene) complex **10'** rather than its *trans*-isomer **10** via a route, *cis*-alkylPd(pyridine) **8** → **10** → TS(**10-10'**) → **10'** → TS(**10'-11'**) →  $\beta$ -agostic *cis*-alkyl complex **11'** with the highest-energy TS(**10'-11'**) of 27.4/27.7 kcal/mol. Our result on this propagation step is in good accordance to the previous study by Ziegler using QM/MM, BP86 for QM part.<sup>14</sup>

In Section 3.3, possible  $\beta$ -hydride elimination from  $\beta$ -agostic *cis*-alkyl complex **9** to Pd(H)(olefin) **12** or the reaction of isomers, from **9'** to **12'**, were studied. In addition to the TS(**9-12**) proposed by Ziegler, here we reported TS(**9'-12'**) with much lower relative energy. For the  $\beta$ -hydride elimination from **9** to **12**, TS(**9-12**) (>37.4/25.3 kcal/mol) should be overcome. In contrast, higher barriers should be overridden in order to reach

$\beta$ -agostic *trans*-alkyl complex **9'**, such as pyridine dissociation TS(**8'-9'**) (29.1/27.4 kcal/mol), *cis*–*trans* isomerization of  $\beta$ -agostic *cis*-alkyl complex **9** TS(**9-9'**) (44.5/31.7 kcal/mol), and ethylene dissociation TS(**10'-9'**) (33.0/30.9 kcal/mol). It is notable that the reactions such as ethylene dissociation or alkyl-isomerization require such high energies. The high barriers to reach **9'** can be attributed to the fact that complex **9'** does have high energy. When the isomer pairs of **8/8'**, **9/9'**, and **10/10'** are compared, the isomers **8'**, **9'**, and **10'** having propyl-groups *trans* to the phosphine are higher in  $\Delta G$  than the isomers **8**, **9**, and **10** having alkyl groups at *trans* to the sulfonate by 10.7, 10.4, and 9.4 kcal/mol, respectively (Figure 8). The difference between the three pairs is rather small. Thus, the high energy of **9'** can be explained by the high-energy nature of the  $\beta$ -agostic alkyl complex compared to that of the four-coordinate species.

In section 3.4, we found that the ethylene insertion to the iso-alkylpalladium species is allowed via a TS (TS(**14'-15'**), 28.6/29.1 kcal/mol) slightly higher in energy than that for the normal alkylpalladium species. The result nicely explains the fact that methyl branches but not any longer branches were detected in the polymerization of ethylene.<sup>13</sup>

In section 3.5, easy chain transfer was suggested to proceed from the more stable PdH(olefin) complex **12'**, if **12'** exists.

According to the results discussed above, the barriers for chain propagation and  $\beta$ -hydride elimination are comparable. Furthermore, after  $\beta$ -hydride elimination, both ethylene insertion into the iso-alkylpalladium complex (branch formation) and chain transfer may be possible. Thus, careful comparison with experiments is necessary to interpret these calculation results correctly.

Experimentally, the following facts are reported.

(1) Linear polyethylene with high molecular weight can be obtained under high pressure of ethylene and reducing ethylene pressure results in lowering the molecular weight of the polymer.<sup>14</sup>

(2) Reducing ethylene pressure resulted in increasing the Me-branch formation.<sup>14</sup>

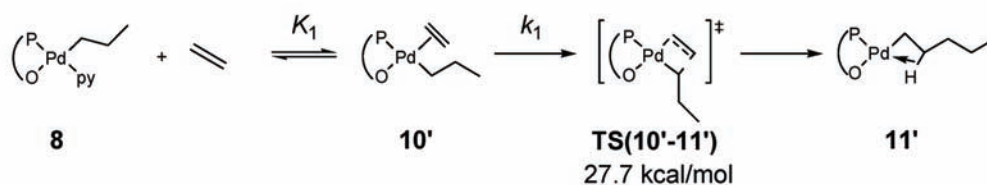
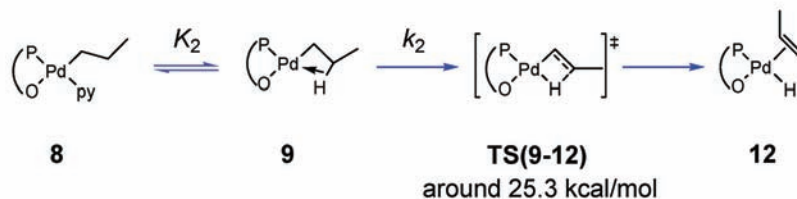
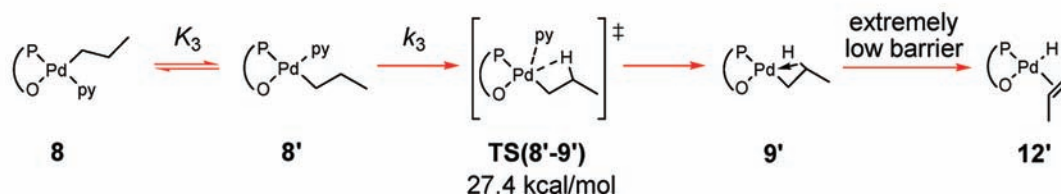
(3) In the absence of ethylene, isomerization of 1-hexene into internal alkenes did occur.

These facts can be interpreted as below using our calculation results.

The molecular weight and the microstructure of the products are qualitatively controlled by the balance of Routes 1–3 in Scheme 11 (the numbers are relative energies to **8** in Gibbs free energy). Route 1 deals with ethylene insertion into the *normal*-alkylpalladium complex which leads to the linear chain propagation. Routes 2 and 3 are the most probable pathways for  $\beta$ -hydride elimination to form the PdH(olefin) complexes **12** and **12'**. Once **12** or **12'** are formed, branched polyethylene can be produced. In addition, formation of **12'** leads to the chain transfer reaction to release low molecular weight product. Thus, the production of linear polyethylene with high molecular weight under high ethylene pressure suggests that **12** and **12'** are merely accessible in the presence of excess amount of ethylene. In fact, among rate equations of these reactions (Routes 1–3), only Route 1, insertion rate, is accelerated by ethylene concentration term (see more details for Supporting Information). Therefore, we conclude that *the Route 1 predominates under the sufficient ethylene pressure while Routes 2 and 3 can occur at the shortage of ethylene.*

Although Ziegler reported that the suppression of  $\beta$ -hydride elimination is the sole reason for the linearity of the polyethylene,<sup>15</sup> they did not consider Route 3 which is indispensable

(31) (a) Andrae, D.; Haeussermann, U.; Dolg, M.; Stoll, H.; Preuss, H. *Theor. Chim. Acta* **1990**, *77*, 123–141. (b) Martin, J. M. L.; Sundermann, A. *J. Chem. Phys.* **2001**, *114*, 3408–3420.

**Scheme 11.** Most Probable Pathways for Ethylene Insertion and  $\beta$ -H Elimination ( $\Delta G$ , based on **8**)<sup>a</sup>**Route 1. Insertion:**  $v_{Route1} = k_1 K_1 a_E a_8 / a_{py}$ **Route 2.  $\beta$ -H elimination to **12**:**  $v_{Route2} = k_2 K_2 a_8 / a_{py}$ **Route 3.  $\beta$ -H elimination to **12'**:**  $v_{Route3} \approx k_3 K_3 a_8$ <sup>a</sup> Introductions of the rate equations are shown in Supporting Information.

for understanding the mechanism of ethylene polymerization catalyzed by Pd phosphine-sulfonate complexes. Moreover, by considering the ethylene concentration, we could precisely interpret the theoretical calculation results in agreement with the experiments.

#### 4. Conclusions

Linear polyethylene propagation on palladium/phosphine-sulfonate was studied both experimentally and theoretically. Experimentally, highly linear polyethylene was obtained with **2a** and **2b**. Formation of a long alkyl-substituted palladium complex **3** was detected as a result of ethylene oligomerization on a palladium center starting from methylpalladium complex **2a**. Additionally, well-defined ethyl and propyl complexes were synthesized as stable *n*-alkyl palladium complexes. In spite of the existence of  $\beta$ -hydrogens, the  $\beta$ -hydride elimination to give 1-alkenes was very slow or negligible in all cases. On the other hand, our observed isomerization of 1-hexene in the presence of the complex **2a** indicated that this catalyst system actually undergoes  $\beta$ -hydride elimination and reinsertion to release internal alkenes, while formation of *normal*-alkylpalladium species was detected during the isomerization process.

The chain-growth, chain-walking, and chain-transfer mechanisms were also studied, theoretically. A unique *cis/trans* isomerization process was proposed for the Pd phosphine-sulfonate system, via the so-called “Berry’s pseudorotation” by the aid of the second oxygen atom of sulfonate group as the associative ligand. The barriers for chain propagation and  $\beta$ -hydride elimination were calculated to be comparable. Once the  $\beta$ -hydride elimination takes place, both ethylene insertion into the *iso*-alkylpalladium complex (branch formation) and chain transfer would be possible. Thus, in the presence of

ethylene pressure, the olefin propagation dominates over  $\beta$ -hydride elimination while  $\beta$ -hydride elimination eventually proceeds at the shortage of ethylene.

#### 5. Experimental Section

**General Methods.** All manipulations were carried out using the standard Schlenk technique under argon purified by passing through a hot column packed with BASF catalyst R3-11. NMR spectra were recorded on a JEOL JNM-ECP500 (<sup>1</sup>H: 500 MHz, <sup>13</sup>C: 126 MHz, <sup>31</sup>P: 202 MHz with digital resolution of 0.239, 0.960, 4.33 Hz, respectively) or a JEOL JNM-ECS400 (<sup>1</sup>H: 400 MHz, <sup>13</sup>C: 101 MHz, <sup>31</sup>P: 162 MHz with digital resolution of 0.09125, 0.767, 3.46 Hz, respectively) NMR spectrometer. Size exclusion chromatography (SEC) analyses at 145 °C were carried out with a Tosoh instrument (HLC-8121) equipped with three columns (Tosoh TSKgel GMHhr-H(20)HT) by eluting the columns with *o*-dichlorobenzene at 1 mL/min. Differential scanning calorimetry was performed on a Mettler DSC 30 instrument. Samples were heated from 50 to 300 °C at a rate of 10 °C/min, and melting points were determined from the data obtained during the second heating run. Fast atom bombardment mass spectrometry (FAB-MS) was carried out on a JEOL JMS-700 spectrometer using PEG calibration and NBA matrix solvent. Dichloromethane, toluene, THF, and hexanes were purified by the method of Pangborn et al.<sup>32</sup> 2-(*o*-methoxyphenyl)phosphino)benzenesulfonic acid (**1a**),<sup>33</sup> 2-(diphenylphosphino)benzenesulfonic acid (**1b**),<sup>34</sup> and {(*o*-MeOC<sub>6</sub>H<sub>4</sub>)<sub>2</sub>P}-C<sub>6</sub>H<sub>4</sub>SO<sub>3</sub>}PdMe(2,6-Me<sub>2</sub>C<sub>5</sub>H<sub>3</sub>N) (**2a**)<sup>7</sup> were prepared according to literature procedures.

(32) Pangborn, A. B.; Giardello, M. A.; Grubbs, R. H.; Rosen, R. K.; Timmers, F. J. *Organometallics* **1996**, *15*, 1518–1520.

(33) Drent, E.; van Dijk, R.; van Ginkel, R.; van Oort, B.; Pugh, R. I. *Chem. Commun.* **2002**, 964–965.

(34) Hearley, A. K.; Nowack, R. A. J.; Rieger, B. *Organometallics* **2005**, *24*, 2755–2763.

**Polymerization of Ethylene.** To a 50 mL autoclave containing Pd complex (0.010 mmol), additive (if any), and a stir bar was transferred 2.5 mL of toluene under argon atmosphere. The mixture was stirred at rt for 10 min and charged with ethylene. The autoclave was heated, and the mixture was stirred. After the reaction, MeOH was added to the cooled contents of the autoclave. Precipitated materials were collected by filtration and washed several times with MeOH. The remaining solid was dried under vacuum at 80 °C to afford polyethylene, which was analyzed without further purification. The number of branches per 1000 carbons was determined by  $^{13}\text{C}$  NMR spectroscopy using inverse-gated decoupling.<sup>35</sup> SEC analysis was performed in *o*-dichlorobenzene at 120 °C.

**Formation of 3 by Reaction of 2a with Ethylene.** A solution of 6.3 mg of **2a** (0.010 mmol) in 0.5 mL of  $\text{CDCl}_3$  was frozen at  $-78$  °C. The NMR tube was removed from the cool bath, and 1 atm of ethylene was quickly introduced to the NMR tube. The mixture was gradually warmed to melt, and the tube was transferred to the NMR probe. The reaction was monitored at 30 °C by  $^1\text{H}$  and  $^{31}\text{P}$  NMR. Formation of **3** was confirmed by  $^1\text{H}$ ,  $^{31}\text{P}$ , and  $^1\text{H}\{^{31}\text{P}\}$  NMR, and HH-COSY.  $^1\text{H}$  NMR (500 MHz,  $\text{CDCl}_3$ ):  $\delta$  0.35–0.52 (m, 4H), 0.67 (tt,  $J = 7.4$ , 7.4 Hz, 2H), 0.82–0.88 (m, 2H), 0.88 (t,  $J = 7.0$  Hz, 3H), 0.93–0.98 (m, 2H), 1.00 (tt,  $J = 7.6$ , 7.6 Hz, 2H), 1.07–1.13 (m, 2H), 1.15–1.20 (m, 4H), 1.25 (s), 1.27–1.31 (m, 2H), 3.21 (s, 6H), 3.59 (s, 6H), 6.90 (dd,  $J = 4.4$ , 8.2 Hz, 2H), 7.06 (dd,  $J = 7.4$ , 7.4 Hz, 2H), 7.11 (d,  $J = 7.8$  Hz, 2H), 7.24 (dddd,  $J = 7.6$ , 7.6, 1.1, 1.1 Hz, 1H), 7.38 (dddd,  $J = 7.6$ , 7.6, 1.1, 1.1 Hz, 1H), 7.45 (ddd,  $J = 11.2$ , 7.8, 1.1 Hz, 1H), 7.48–7.51 (m, 2H), 7.57 (t,  $J = 7.7$  Hz, 1H), 7.89 (br s, 2H), 8.12 (ddd,  $J = 7.8$ , 4.8, 1.1 Hz, 1H).  $^{31}\text{P}$  NMR (202 MHz,  $\text{CDCl}_3$ ):  $\delta$  23.5.  $^1\text{H}\{^{31}\text{P}\}$  NMR showed that in the alkyl region of the  $^1\text{H}$  NMR spectrum,  $^{31}\text{P}$ -decoupling essentially only changed the shape of the multiplet at 0.93–0.98 ppm to a triplet ( $J = 8.0$  Hz) at 0.96 ppm in the alkyl region of the  $^1\text{H}$  NMR spectrum. Therefore, this peak was assigned to the signal of the methylene directly bonded to the palladium. The HH-COSY spectra revealed the connectivity of methylenes not giving signals at 1.25 ppm and the signals of terminal ethyl group of the *n*-alkyl chain. *n*-Alkyl group is assigned to be located at the *cis*-position to the phosphorus atom due to strong *trans*-influence of alkyl group and phosphine and structural similarity to **2a**.

Palladium complex with a long alkyl chain **3** can also be generated by performing the reaction in a Schlenk flask. To a solution of 19 mg of **2a** (0.030 mmol) in 2.5 mL of  $\text{CHCl}_3$  was introduced 1 atm of ethylene. The reaction was monitored by  $^1\text{H}$  and  $^{31}\text{P}$  NMR by taking a small fraction of the solution, evaporating the solvent, and dissolving the residue in  $\text{CDCl}_3$ . Formation of **3** was confirmed by  $^1\text{H}$  and  $^{31}\text{P}$  NMR (>90% conversion after 200 min). No free ethylene or coordinated ethylene was observed by  $^1\text{H}$  NMR.

**Synthesis of  $[\{o\text{-(Ph}_2\text{P)C}_6\text{H}_4\text{SO}_3\}\text{PdMe(py)}]$  (**2b**).** A solution of 2-(diphenylphosphino)benzenesulfonic acid (**1b**) (0.342 g, 1.00 mmol) and (tmeda)PdMe<sub>2</sub> (0.252 g, 1.00 mmol) in  $\text{CH}_2\text{Cl}_2$  (15 mL) was cooled to  $-78$  °C and stirred for 15 min. Pyridine (0.41 mL, 5.0 mmol) was added dropwise. The mixture was stirred at  $-78$  °C for 30 min, warmed to room temperature, and stirred for 80 min. The resulting solution was concentrated to  $\sim 5$  mL and added dropwise to 60 mL of hexane. The precipitate was collected by filtration and washed with hexane. The compound was purified by recrystallization from  $\text{CH}_2\text{Cl}_2$  to afford white powder (209 mg, 38.5% yield); mp: 162 °C dec; IR (KBr)  $\text{cm}^{-1}$ : 3059, 1437, 1269, 1167, 1113, 1001, 745, 673;  $^1\text{H}$  NMR (500 MHz,  $\text{CDCl}_3$ ):  $\delta$  0.50 (d,  $J = 2.5$  Hz, 3H), 7.04 (ddd,  $J = 1.1$ , 7.8, 10.1 Hz, 1H), 7.35 (ddd,  $J = 1.1$ , 1.1, 7.7 Hz, 1H), 7.42–7.55 (m, 9 H), 7.58–7.65 (m, 4H), 7.85 (dd,  $J = 7.6$ , 7.6 Hz, 1H), 8.28 (ddd,  $J = 1.4$ , 4.4, 7.8 Hz, 1H), 8.79 (d,  $J = 4.8$  Hz, 2H);  $^{13}\text{C}$  NMR (101 MHz,

$\text{CDCl}_3$ ):  $\delta$  0.7 (d,  $J = 5$  Hz), 125.0 (s), 128.4 (d,  $J = 49$  Hz), 128.6 (s), 128.7 (d,  $J = 12$  Hz), 129.8 (d,  $J = 7$  Hz), 129.9 (d,  $J = 55$  Hz), 130.9 (d,  $J = 3$  Hz), 131.1 (d,  $J = 3$  Hz), 134.2 (d,  $J = 12$  Hz), 134.5 (d,  $J = 2$  Hz), 138.3 (br), 149.3 (d,  $J = 13$  Hz), 150.2 (br);  $^{31}\text{P}$  NMR (202 MHz,  $\text{CDCl}_3$ ):  $\delta$  28.7. The white powder included  $\text{CH}_2\text{Cl}_2$  (7 mol %) and absorbed water (8 mol %), which is confirmed by  $^1\text{H}$  NMR. Anal. Calcd for  $\text{C}_{24}\text{H}_{22}\text{NO}_3\text{PPdS} + 7\%$   $\text{CH}_2\text{Cl}_2 + 8\%$   $\text{H}_2\text{O}$ : C, 52.63; H, 4.09; N, 2.55. found: C, 52.63; H, 4.17; N, 2.56.

**Synthesis of  $[\text{Pr}_2\text{EtNH}]\{[o\text{-(}o\text{-MeOC}_6\text{H}_4)_2\text{P}]\text{C}_6\text{H}_4\text{SO}_3\}\text{PdCl}_2]$  (**5**).** To a solution of 0.614 g of **1a** (1.53 mmol) in 20 mL of  $\text{CH}_2\text{Cl}_2$  was added 2.8 mL (16 mmol) of  $\text{Pr}_2\text{EtN}$ , and the mixture was stirred for 10 min at rt.  $\text{PdCl}_2(\text{cod})$  (0.461 g, 1.61 mmol) was added to a mixture and stirred for 1.5 h at rt. The resulting solution was filtered through Celite, concentrated and reprecipitated with hexane. The residual solid was washed with hexane and ether. The volatiles were removed in vacuo to afford a yellow powder (407 mg, 57.4% yield). mp: 129 °C dec; IR (KBr)  $\text{cm}^{-1}$ : 2986, 1588, 1477, 1273, 1161, 1020, 988, 762;  $^1\text{H}$  NMR (400 MHz,  $\text{CDCl}_3$ ):  $\delta$  1.47 (d,  $J = 6.6$  Hz, 6H,  $\text{HNCH}(\text{CH}_3)_2$ ), 1.55–1.64 (m, 9H,  $\text{HNCH}_2\text{CH}_3$ ,  $\text{HNCH}(\text{CH}_3)_2$ ), 3.19–3.28 (m, 2H,  $\text{HNCH}_2\text{CH}_3$ ), 3.67 (s, 6H,  $\text{CH}_3\text{OC}_6\text{H}_4$ ), 3.83–3.92 (m, 2H,  $\text{HNCH}(\text{CH}_3)_2$ ), 6.88 (dd,  $J = 8.4$ , 5.0 Hz, 2H), 7.04 (dd,  $J = 7.3$ , 7.3 Hz, 2H), 7.28–7.36 (m, 2H), 7.44–7.49 (m, 1H), 7.52 (dd,  $J = 7.8$ , 7.8 Hz, 2H), 7.98 (dd,  $J = 7.4$ , 4.4 Hz, 1H), 8.12 (br, 2H), 9.24 (br, 1H, NH);  $^{13}\text{C}$  NMR (126 MHz,  $\text{CDCl}_3$ ):  $\delta$  12.0 (s,  $\text{HNCH}_2\text{CH}_3$ ), 17.6 (s,  $\text{HNCH}(\text{CH}_3)_2$ ), 18.9 (s,  $\text{HNCH}(\text{CH}_3)_2$ ), 42.1 (s,  $\text{HNCH}_2\text{CH}_3$ ), 54.0 (s,  $\text{HNCH}(\text{CH}_3)_2$ ), 55.7 (s,  $\text{CH}_3\text{OC}_6\text{H}_4$ ), 111.5 (d,  $J = 5$  Hz), 120.7 (d,  $J = 13$  Hz), 126.7 (d,  $J = 9$  Hz), 127.8 (d,  $J = 33$  Hz), 128.7 (d,  $J = 8$  Hz), 130.2 (d,  $J = 2$  Hz), 130.4 (d,  $J = 3$  Hz), 133.9 (d,  $J = 2$  Hz), 134.6 (s), 134.7 (d,  $J = 15$  Hz), 138.6 (br d), 160.3 (s);  $^{31}\text{P}$  NMR (202 MHz,  $\text{CDCl}_3$ ):  $\delta$  3.93; HRMS-FAB ( $m/z$ ):  $[\text{M} + \text{Pr}_2\text{EtNH}]^+$  calcd for  $\text{C}_{36}\text{H}_{58}\text{Cl}_2\text{N}_2\text{O}_5\text{PPdS}$ , 837.2166; found, 837.2247.

**Synthesis of  $[\{o\text{-(}o\text{-MeOC}_6\text{H}_4)_2\text{P}]\text{C}_6\text{H}_4\text{SO}_3\}\text{PdCl}_2(2,6\text{-Me}_2\text{C}_5\text{-H}_3\text{N})]$  (**4**).** To a solution of 0.496 mg of **5** (0.714 mmol) in 30 mL of  $\text{CH}_2\text{Cl}_2$  were added 0.744 mg of  $\text{NaBARf}_4$  (0.840 mmol) and 97.8  $\mu\text{L}$  (0.867 mmol) of 2,6-lutidine, and the mixture was stirred for 5 h at rt. The solution was filtered through Celite. The solvent was removed in vacuo, and the resulting solid was washed with hexane and methanol. The precipitate was filtered and dried in vacuo to afford a yellow solid (270 mg, 59.3% yield). mp: 162 °C dec; IR (KBr)  $\text{cm}^{-1}$ : 1589, 1466, 1283, 1163, 982, 768.;  $^1\text{H}$  NMR (500 MHz,  $\text{CDCl}_3$ ):  $\delta$  3.38 (s, 6H,  $\text{CH}_3$  of lutidine), 3.65 (s, 6H,  $\text{CH}_3\text{OC}_6\text{H}_4$ ), 6.93 (dd,  $J = 8.3$ , 5.1 Hz, 2H), 7.06–7.14 (m, 4H), 7.30–7.37 (m, 2H), 7.47–7.60 (m, 4H), 8.02 (br, 1H), 8.06 (dd,  $J = 6.3$ , 6.3 Hz, 2H);  $^{13}\text{C}$  NMR (101 MHz,  $\text{CDCl}_3$ ):  $\delta$  25.5 (s,  $\text{CH}_3$  of lutidine), 55.2 (s,  $\text{CH}_3\text{OC}_6\text{H}_4$ ), 111.0 (d,  $J = 5$  Hz), 113.8 (d,  $J = 65$  Hz), 120.9 (d,  $J = 13$  Hz), 122.9 (d,  $J = 4$  Hz), 126.6 (d,  $J = 55$  Hz), 127.3 (d,  $J = 9$  Hz), 128.7 (d,  $J = 9$  Hz), 130.7 (d,  $J = 2$  Hz), 134.1 (d,  $J = 2$  Hz), 134.3 (d,  $J = 2$  Hz), 138.1 (d,  $J = 12$  Hz), 138.6 (s), 146.1 (d,  $J = 13$  Hz), 159.0 (s), 160.1 (s);  $^{31}\text{P}$  NMR (162 MHz,  $\text{CDCl}_3$ ):  $\delta$  3.15. These NMR data are consistent with that of the crystals obtained by the reaction of **3** with  $\text{CDCl}_3$  (*vide supra*). See Supporting Information for X-ray analysis of **4**.

**Generation of  $[\{o\text{-(}o\text{-MeOC}_6\text{H}_4)_2\text{P}]\text{C}_6\text{H}_4\text{SO}_3\}\text{PdEt}(2,6\text{-Me}_2\text{C}_5\text{-H}_3\text{N})]$  (**6Et**).** To a solution of 75.0 mg of **4** (0.10 mmol) in 15 mL of toluene was added 1.2 equiv of triethylaluminum hexane solution, and the mixture was stirred for 3 h at rt. The solution was filtered through Celite. The solvent was removed in vacuo and extracted with hexane. The precipitate was filtered and dried in vacuo to afford **6Et** as a yellowish white powder (22 mg) containing 11 mol % of **4**. **6Et**:  $^1\text{H}$  NMR (500 MHz,  $\text{CDCl}_3$ ):  $\delta$  0.00 (td,  $J = 7.5$ , 4.6 Hz, 3H), 1.02 (dq,  $J = 14.4$ , 7.2 Hz, 2H), 3.20 (s, 6H), 3.58 (s, 6H), 6.90 (dd,  $J = 8.1$ , 4.3 Hz, 2H), 7.05 (dd,  $J = 7.3$ , 7.3 Hz, 2H), 7.10 (d,  $J = 7.6$  Hz, 2H), 7.22–7.27 (m, 1H), 7.32–7.45 (m, 2H), 7.49 (dd,  $J = 7.9$ , 7.9 Hz, 2H), 7.55 (dd,  $J = 7.6$ , 7.6 Hz, 1H), 7.85 (br, 2H), 8.12 (ddd, 7.7, 7.9, 1.0 Hz, 1H);  $^{13}\text{C}$  NMR (126

(35) Cotts, P. M.; Guan, Z.; McCord, E.; McLain, S. *Macromolecules* **2000**, *33*, 6945–6952.

MHz, CDCl<sub>3</sub>):  $\delta$  12.1, 16.1, 26.0, 54.9, 114.3, 121.1, 128.1, 129.8, 130.1, 132.6, 133.1, 136.4, 157.7; <sup>31</sup>P NMR (202 MHz, CDCl<sub>3</sub>):  $\delta$  23.0.

**Generation of [(*o*-MeOC<sub>6</sub>H<sub>4</sub>)<sub>2</sub>P]C<sub>6</sub>H<sub>4</sub>SO<sub>3</sub>PdPr(2,6-Me<sub>2</sub>C<sub>5</sub>-H<sub>3</sub>N)] (6<sub>Pr</sub>).** To a solution of 75.0 mg of **4** (0.10 mmol) in 15 mL of toluene was added 0.30 equiv of tripropylaluminum toluene solution, and the mixture was stirred for 1 h at rt. The solution was filtered through Celite. The solvent was removed in vacuo and extracted with hexane. The precipitate was filtered and dried in vacuo to afford **6Pr** as a white powder (55 mg) containing 8 mol % of **4**. **6Pr**: <sup>1</sup>H NMR (500 MHz, CDCl<sub>3</sub>):  $\delta$  0.17 (t, *J* = 7.1 Hz, 3H), 0.43–0.54 (m, 2H), 0.93 (dt, *J* = 11.0, 5.1 Hz, 2H), 3.20 (s, 6H), 3.57 (s, 6H), 6.90 (dd., *J* = 8.2, 4.4 Hz, 2H), 7.06 (dd, *J* = 7.3, 7.3 Hz, 2H), 7.11 (d, *J* = 7.8 Hz, 2H), 7.21–7.28 (m, 1H), 7.38 (dd, *J* = 7.6, 7.6 Hz, 1H), 7.45 (dd, *J* = 11.2, 8.0 Hz, 1H), 7.50 (dd, *J* = 7.7, 7.7 Hz, 2H), 7.56 (dd, *J* = 7.7, 7.7 Hz, 1H), 7.90 (br, 2H), 8.13 (ddd, *J* = 7.6, 4.8, 0.9 Hz, 1H); <sup>13</sup>C NMR (126 MHz, CDCl<sub>3</sub>):  $\delta$  15.9 (*J*<sub>P-C</sub> = 4 Hz), 21.1, 24.4, 114.4, 121.0, 129.8, 130.1, 133.1, 136.0, 158.9; <sup>31</sup>P NMR (202 MHz, CDCl<sub>3</sub>):  $\delta$  23.2.

**Lutidine addition to 3.** Complex **3** could be also prepared from **6Pr** with ethylene in the same procedure as from **2a**. To a solution of **4** (13 mg, 0.016 mmol) in toluene (10 mL), was added 0.20 equiv of tripropylaluminum (3.5  $\mu$ L of 0.1 M toluene solution). After stirring under Ar for 20 min, the solution was filtered through a pad of Celite. The solvents were removed *in vacuo* to give a crude mixture of **6Pr**. Propyl complex **6Pr** thus obtained was dissolved in 0.5 mL of CDCl<sub>3</sub> and treated with ethylene under atmospheric pressure for 9 h at room temperature to afford **3**. The formation of **3** was confirmed by <sup>1</sup>H and <sup>31</sup>P NMR spectroscopy. Upon addition of 1.9  $\mu$ L of 2,6-lutidine to this solution, the peak at 0.05 ppm in <sup>1</sup>H NMR chart disappeared as demonstrated in Supporting Information.

**Isomerization experiment.** To a solution of complex **2a** (0.020 mmol) in 0.5 mL of CDCl<sub>3</sub> was added 13 equivalent amounts of 1-hexene via syringe. The tube was sealed with screw cap, stored in an NMR probe under 60 °C, and monitored by NMR. After 19 h at 60 °C, 63% (7.8 mmol) of the 1-hexene converted to internal olefins as shown in Supporting Information.

**Theoretical Methods.** All geometries of the reactants, intermediates, transition states, and products of the reactions were fully

optimized by using the Gaussian 03 program,<sup>36</sup> and the B3LYP<sup>19</sup> method with combined basis sets (Lanl2dz basis sets and effective core potential for the palladium atom<sup>20</sup> and 6-31G(d) basis sets for the other atoms). Harmonic vibration frequency calculations at the same level were performed to verify all stationary points as local minimum (with no imaginary frequency) or transition state (with one imaginary frequency). IRC calculations<sup>37</sup> were also performed.

**Acknowledgment.** We are grateful to Assoc. Prof. Y. Nishibayashi and Dr. Y. Miyake at the University of Tokyo for high-resolution FAB-MS analysis of **5**. Computer resources for theoretical calculation were mainly provided by the Research Center for Computational Science in the National Institutes of Natural Sciences. This work was supported by the Global COE Program for Chemistry Innovation. A.N. is grateful to the Japan Society for the Promotion of Science (JSPS) for a Research Fellowship for Young Scientists. LWC acknowledges the Fukui Institute Fellowship. This work is in part supported by Japan Science and Technology Agency (JST) with a Core Research for Evolutional Science and Technology (CREST) grant in the Area of High Performance Computing for Multiscale and Multiphysics Phenomena.

**Supporting Information Available:** Complete citation of reference 36, results of ethylene polymerization (Table S-1), NMR charts for **2b**, **3**, **4**, **5**, **6E**, **6Pr** (Figures S1–S10, S-13–15), NMR studies on the reaction of **3** with lutidine (Figure S-11), expansion of Figure 4 (Figure S-12), crystal data for **4** (Tables S2–S8 and Figure S-16), optimized structures for all intermediates with simplified ligand (Figure S-17), Cartesian coordinates of optimized species (Table S-7). This material is available free of charge via the Internet at <http://pubs.acs.org>.

JA9047398

(36) Frisch, M. J.; et al. *Gaussian 03*, Revision C02; Gaussian, Inc.: Wallingford, CT, 2007.

(37) (a) Gonzalez, C.; Schlegel, H. B. *J. Chem. Phys.* **1989**, *90*, 2154–2161. (b) Gonzalez, C.; Schlegel, H. B. *J. Phys. Chem.* **1990**, *94*, 5523–5527.